NUMERICAL DEVELOPMENT OF UNSTEADY VORTEX-LATTICE METHOD EXPANSION FOR LEADING-EDGE SHEDDING PREDICTION WITH EXPERIMENTAL VALIDATION

Monteiro, T. P. *, Ramesh, K., Silvestre, F.***
***Instituto TecnolÃşgico de Aeronautica, Brazil , **University of Glasgow, UK**

Keywords: *Aerodynamics, Aeroelasticity, Wind Tunnel*

Abstract

With a steady grow in fuel emissions and flight efficiency requirements, airplanes are being developed with higher aspect ratios and lighter materials. This increases overall flexibility, and requires more advanced aerodynamic and structural models. The Unsteady Vortex-Lattice Method (UVLM) has been successfully used for these cases, however one of its shortcommings is it lacks the ability to model leading-edge stall. This work shows the ongoing development of an expanded UVLM, capable of predicting leading-edge vortex shedding and its application to flexible aircraft. The model is validated against experimental wind-tunnel tests of a flat plate undergoing prescribed movement and flutter limit-cycle oscillations.

1 Introduction

Higher aspect ratios and lighter materials seek to reduce fuel emissions and increase flight efficiency by reducing lift to drag ratio and overall weight, respectively, of the aircraft. In particular, High-Altitude Long Endurance (HALE) aircaft tend to have this characteristics as their main engineering feature.

A number of modern aircraft, for example the F-16s, have been exposed to flutter conditions, and limit-cycle oscillations (LCOs) where obeserved when nonlinearities on the system, such as geometric, structure and aerodynamic, acted to limit the motion amplitude [3]. This, with the recent trend in design of higher aspect ratios and lighter materials, have created instances where rigid-body and aeroelastic dynamics are coupled and need to be taken into account together.

Flutter, in this cases, is usually modeled with linear analysis, however LCOs are by their very nature nonlinear. This inability to model LCOs results in extensive, and expensive, flight testing. These nonlinearities can be of structural or aerodynamic nature, with structural nonlinearity rising from large deformations, material properties, or loose linkages, whereas aerodynamic nonlinearities results from compressibility or viscous effects. This work focus on aerodynamic nonlinearities[1].

The Unsteady Vortex-Lattice Method (UVLM) is a three-dimensional aerodynamic model based on potential-flow formulation that shows great promise to model nonlinear aerodynamics due to its ability to model nonplanar wakes. The computational cost of this method sits between linear models such as Doublet-Lattice Method, and high-fidelity ones such as Computation Fluid Dynamics, making it an ideal candidate for HALE aircraft[2].

By dynamically modeling the wake at each time-step, it can account for large, and fast movements, however, flow separation is still a limitation. In particular, Leading-Edge flow separation has been proven to be major contributor to

LCOs[3].

Ramesh et al[1], has developed a two-dimensional method that, by using leading-edge suction as a modulator, can predict leading-edge flow separation and shed leading-edge vortices (LEV) into the flow, effectively modeling LCOs on an airfoil, this method was called Lesp-Modulated Discrete Vortex Method (LDVM). This method is currently being expanded to 3D cases using a strip theory approach, with promising results[3].

An UVLM implementation that combines LDVM's leading-edge vortexes and UVLM was proposed by Hirato [4]. With special attention to the numerical accuracy and stability, this work proved that it was possible to add LDVM's LESP modulation to UVLM with good results.

This work expands the findings Hirato, proposing a matrix-based way to calculate the Leading-Edge Vortex Modulator in UVLM. This work also seeks to validate LESP-Modulation against wind tunnel test results for prescribed flexible body movement and coupled structural/aerodynamic flutter. LDVM results were also used to validate the new model.

2 Model Development

2.1 Aerodynamic Model

The current UVLM model was based on Katz and Plotkin [4] implementation, with an expansion to calculate the LESP for each chordwise strip following the two-dimensional panel method presented in the previous section. The implementation was done in the MATLAB environment, with extensive use of C code generation technology to speed up simulation time.

Katz and Plotkin[4] model calculates the bound vortex distribution by a system of equations (1), where the right-hand side (RHS) is the normal velocity contribution from the developed wake and the wing kinematics, and the a_{ij} coefficients are the calculated as the influence of unit bound vortexes rings in each other.

$$\begin{pmatrix} a_{11} & a_{12} & \cdots & a_{1m} \\ a_{21} & a_{22} & \cdots & a_{2m} \\ \vdots & \vdots & \ddots & \vdots \\ a_{m1} & a_{m2} & \cdots & a_{mm} \end{pmatrix} \begin{pmatrix} \Gamma_1 \\ \Gamma_2 \\ \vdots \\ \Gamma_m \end{pmatrix} = \begin{pmatrix} RHS_1 \\ RHS_2 \\ \vdots \\ RHS_m \end{pmatrix} \tag{1}$$

Where,

$$m = M_{panelRows} * N_{panelCollumns} \tag{2}$$

From the bound vortex distribution, it is possible to calculate the pressure distribution at each panel. Equation 2 calculates the force vector at each panel, with the third element of the vector representing the Lift force.

$$\begin{aligned} \Delta \mathbf{F}_{ij} = \\ \rho([U(t)+u_W, V(t)+v_W, W(t)+w_W]_{ij} \cdot \tau_i \frac{\Gamma_{i,j}-\Gamma_{i-1,j}}{\Delta c_{ij}} \\ +[U(t)+u_W, V(t)+v_W, W(t)+w_W]_{ij} \cdot \tau_j \frac{\Gamma_{i,j}-\Gamma_{i,j-1}}{\Delta b_{ij}} \\ + \frac{\delta}{\delta t}\Gamma_{ij})\Delta S_{ij}\mathbf{n}_i j \end{aligned} \tag{3}$$

Where $[U(t), V(t), W(t)]$ is the kinematic contribution, $[u_W, v_W, w_W]$ is the wake contribution, τ_i and τ_j are the tangent unit vector chordwise and spanwise, respectively. Δc_{ij} and Δb_{ij} are the panel sizes, chordwise and spanwise respectively. Finally, ρ is the air density, ΔS_{ij} is the panel area and $\mathbf{n}_{ij}$ is the normal vector at the panel. Lift and Moment coefficients were calculated for each spanwise location by combining the forces and moments of every chordwise panel. Equations 3 and 4 show how the lift and moment coefficient calculation for each spanwise location.

$$C_{Lj} = \frac{\sum \Delta F(3)_{ij}}{q_\infty S_1} \tag{4}$$

$$C_{Mj} = \frac{\sum L * (x_j^{pvt} - x_{ij}^{\Gamma})}{q_\infty c S_1} \tag{5}$$

Where the x_j^{pvt} is the aerodynamic pivot position for the spanwise position j, x_{ij}^{Γ} is the vortex ring position at the panel, and q_∞ is the dynamic pressure.

From the model developed by Hirato, Y[4] we can calculate an approximation for A_0 from the leading-edge panel circulation. This approximation is empirically determined and will be applied to the current model. It is currently under development a more robust, and efficient, way of calculating the A0 is under development to reuse some of the assets already calculated by UVLM. Equation 3 gives the A_0 for each strip in the wing.

$$A_0(t,y_j) = \frac{1.13\Gamma_1(t,y_j)}{U_\infty c[cos^{-1}(1-\frac{2\Delta x}{c})+sin(cos^{-1}(1-\frac{2\Delta x}{c}))]} \quad (6)$$

This approach to the solution proved well suited for panel based methods, not requiring a finer mesh, and providing a good approximation for the A_0.

2.2 Structural Model

Two structural models were used to verify the proposed UVLM changes against the experiments: The first model, presents a controlled first bending mode deflection, allowing for the modeling of the prescribed results. The second was a coupled structural model to allow the modeling of flutter condition. In both cases, integration was made around changes to the local grid used in UVLM, with the elastic displacements happening around the local axis.

2.2.1 Prescribed Motion Structural Model

For the prescribed motion model, Bisplinhoff R.[6] provides a good approximation for the first mode shape of a cantilever beam. This type of model is considered an uncoupled model: Positions and deformations are defined as a vector in time and aerodynamic forces and moments are calculated without acting on the structure. Equation 4 gives the vertical displacement of a point in the wing span.

$$h(y) = D[(\frac{\sin(\sqrt{\frac{w_n}{a}}b)-\sinh(\sqrt{\frac{w_n}{a}}b)}{\cosh(\sqrt{\frac{w_n}{a}}b)+cos(\sqrt{\frac{w_n}{a}}b)}) (\sinh(\sqrt{\frac{w_n}{a}}y)-\sin(\sqrt{\frac{w_n}{a}}y)) + (\cosh(\sqrt{\frac{w_n}{a}}y)-cos(\sqrt{\frac{w_n}{a}}y))] \quad (7)$$

Where,

$$a = \sqrt{\frac{EI}{m}} \quad (8)$$

In equation 5, E is the elastic coefficient, I the wing Inertia and m is the mass. The parameter D from Equation 4 can be obtained by applying the equation o a known condition, in this case, the maximum measured wing tip displacement.

2.2.2 Flutter Structural Model

For flutter prediction and simulation, a coupled model is required. A modal superposition approach can be used to great effect in calculating the deformations in the wing and coupling it to the aerodynamic forces calculated by UVLM.Writing the physical coordinates as equation 6, it is possible to express the deformations as a combinations of modal shapes. These can be truncated to allow for a order reduction and fast executing code.

$$q = \phi\eta \quad (9)$$

Where ϕ is the eigenvector matrix representing the modal shapes and η is the generalized displacements. The equations of motion can be rewritten as:

$$\ddot{\eta}_{mx1} + 2\varepsilon_{mxm}\omega_{n_{mxm}}\dot{\eta}_{mx1} + \omega^2_{n_{mxm}}\eta_{mx1} = \mu^{-1}_{mxm}Q_{mx1} \quad (10)$$

With m being the number of modes used at the truncation, ε being the diagonal matrix of modal damping, ω_n the diagonal matrix of modal natural frequencies, μ the diagonal matrix of modal masses and Q the vector of generalized forces.

The generalized forces Q can be written as a function of C_L and C_M, both calculated by the UVLM model. Equation 8 shows generalized forces calculation.

$$Q = \phi q_\infty \begin{bmatrix} -C_L c \Delta y \\ C_M c^2 \Delta y \\ 0 \end{bmatrix} \tag{11}$$

3 Wind Tunnel Experiments

Initial experiments were developed to verify aerodynamic nonlinearities caused by leading edge vortex formation in a flat plate. Two base tests were developed: the first test representing a prescribed movement with leading-edge vortex influence, and a the second test representing a flutter condition with Limit-Cycle Oscillations[2].

Following the results obtained before [2], both tests were expanded with a velocity sensor positioned to measure the trailing edge velocity during the prescribed motion and flutter oscillations. More advanced signal conditioners were also used to mitigate inacuracies in the force measurement.

Figure 01 shows the prescribed test setup, composed by a flat plate with a PZT actuator mounted on top of a balance device in front of a wind-tunnel, the DSpace data acquisition system, and the laser velocity sensor.

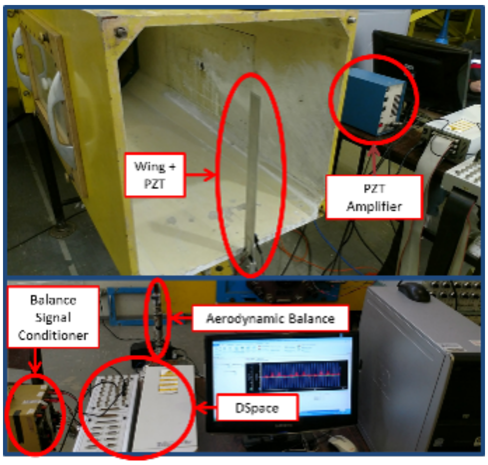

Figure 01: Prescribed Test Setup

3.1 Prescribed Movement Tests

The prescribed movement test used the flat plate, positioned against a steady free-flow of 10 m/s at several angles of attack. Measurements were performed for at a steady-state static situation and with the flat plate excited by PZT actuators attached to its root. These PZTs, when activated close to the plate's natural frequency for the first bending mode, generated a high amplitude bending motion, that combined with the freestream, produces high apparent angle of attack. Figure 02 shows a schematic of the test.

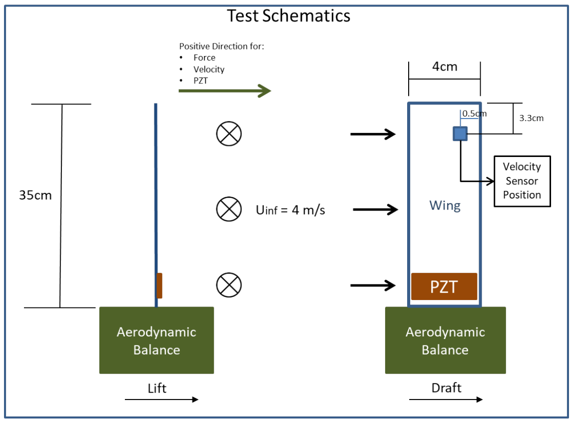

Figure 02: Experimental Test Schematic

These tests were executed by achieving the 10 m/s freestream velocity, and then measuring the static, steady-state, condition, followed by the dynamic prescribed movement. For this article. Results from three angles of attack will be used to verify the UVLM model calibration to expected LEV formation.

3.2 Flutter Condition Tests

The Flutter condition test was designed to visualize Leading-Edge Vortices influence when Limit-Cycle Oscillations are achieved. Several flat plates, with a ballast, where tested. The ballast was positioned to lower the flutter velocity and allow it to occur inside the tunnels operational speed. Figure 03 shows the flutter test setup.

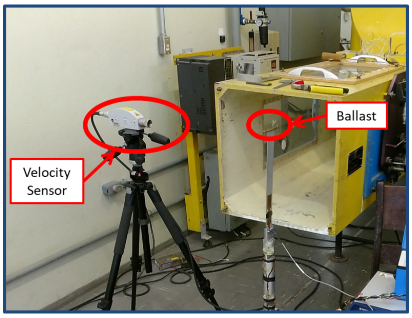

Figure 03: Flutter Test Setup

Tests consisted of increasing the tunnel velocity until flutter was perceived. The velocity was them kept until Limit-Cycle Oscillations are sustained.

A more flexible wing was eventually selected for the flutter tests, this was intended to reduce simulation time by requiring a lower freestream velocity to achieve flutter. This wing has the dimensions of 0.4m for span, 0.027m chord and the same 0.8mm for thickness.

During the tests, it was observed coupling between the wing's and balance's modes of vibration. Different wings presented different couplings, and, although lift readings presented some distortions, trailing edge velocity was successfully captured by the measurement apparatus.

4 Results

Static Tests were run at the wind tunnel to verify the correlation between lead edge vortexes and high angles of attack. For the Aluminum flat plate, a angle of attack sweep was performed from 0 to 11 degrees. Figure 04, show that after 6 degrees of angle of attack a nonlinear response is observed.

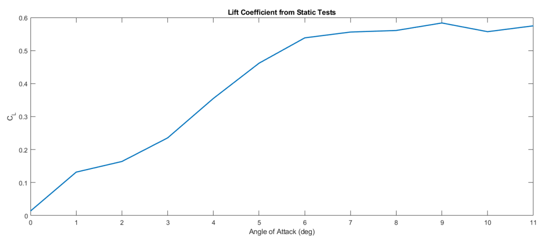

Figure 04: Static angle of attack test sweep

By running the static test with UVLM and LDVM for a seven degree angle of attack, it is possible to verify that this condition should indeed have Lead-Edge Vortex generation. The reference value of 0.1 for LEV was defined in [1] for flat plates. Figure 05, shows good relationship between the UVLM and LDVM results for A0 estimation.

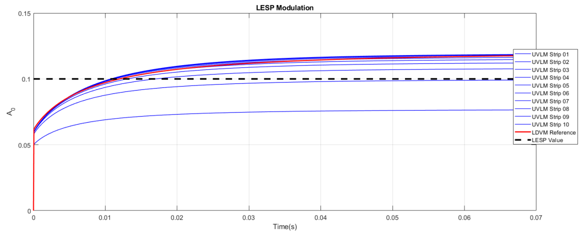

Figure 05: LESP Static Test

Two important aspects are important to notice:

1. Due to UVLM's 3D implementation, there is a reduced circulation, and therefore A_0 at the wing tip. This explains the different values between each strip, with the strips close to the tip showing reduced values.

2. UVLM A_0 calculation, as of implemented, is an approximation based on previous tests[4].

When analyzing the prescribed motion results, with a initial angle of attack of 7 degrees, it is possible to notice that UVLM doesn't achieve the C_L values measured at aerodynamic balance (figure 06 - right). This is consistent with the results obtained by Ramesh, et al [3] that also found greater values from the experiments, with the mainreason being that we have inertial forces that are captured by the balance and are not easily modeled.

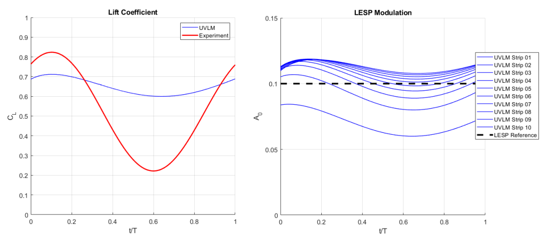

Figure 06: Prescribed Test Results

We also can verify that the experiment is bound to have LEV generated by all strips (figure 06 - left). This would also increase the lift force generated at the strips and could account for the difference in the results.

Simulating flutter presented an extra difficult in requiring longer simulations to verify the vibration development through time. However, greater velocity and using more flexible wings, with smaller chords, impacts the time step needed to achieve a stable simulation on UVLM.

For the more flexible flat plate with a ballast in a 5mm offset, flutter was obtained with a 10m/s freestream velocity, and one degree angle of attack (figure 07).

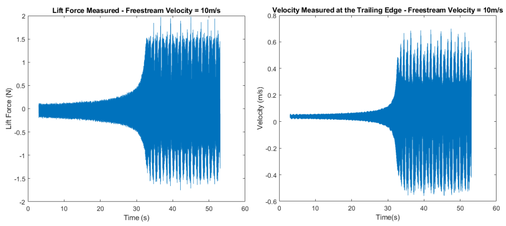

Figure 07: Flutter Test Results

It is possible to verify, from the coupled simulation results, that initial deformation is dominated by the first elastic mode (η_1), with the second and third modes (η_2 and η_3 respectively), that will eventually develop into the LCO, initially with smaller magnitude, but with clear increase in magnitude through time (figure 08).

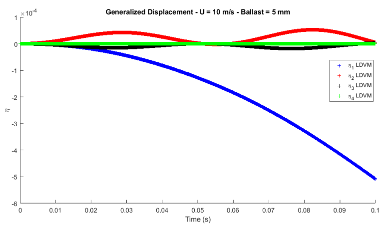

Figure 08: Generalized Modes Displacements

When analyzing the dynamics of the wing tip together with the A_0 (figure 09), we can see on the left graphic that the angle of attack starts a fast harmonic movement, with the plunge, on the ,middle figure, presenting a higher amplitude and lower frequency behavior. From the right graphic it is possible to verify that the wing tip is still under the LESP threshold, however with a clear upward trend, it is expected from test results and linear simulations that the movement slowly increases in amplitude until LEVs are shed and the dynamics migrate to the LCO condition.

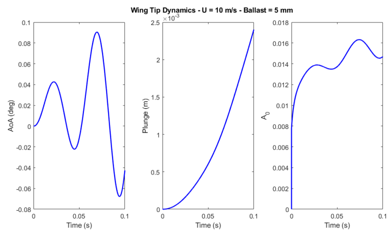

Figure 09: Wing Tip Strip Dynamics

Unfortunately, longer simulations were not possible due to the slow simulation time, that hinder current model applications to initial verifications. Future developments will apply parallel computing capabilities to speed-up simulation and allow for longer simulations. This will be essential to allow for LEV generation.

5 Conclusions and Next Steps

Static tests showed a correlation between LESP based LEV generation and angle of attack. Further investigations should be performed to verify if LEV generation will be enough to reproduce the nonlinear behavior resulting from static-stall condition.

Uncoupled models were used to validate and verify A_0 calculation in UVLM, with good correlation between 2D and 3D models. Comparisons with wind tunnel results show that LEV generation should be expected and can happen unevenly spanwise.

Coupled models show wing deformation's influence on A_0 and should be able to represent flutter scenarios. Future LEV implementation is necessary however to achieve LCO.

However, faster models will be necessary to achieve feasible simulation time and performance. The test results currently available should be useful in calibrating and validating LEV generation.

5.1 References

References

[1] Ramesh K, et al. Discrete-vortex method with novel shedding criterion for unsteady airfoil flows with intermittent leading-edge vortex shedding. *Journal of Fluid Mechanics*, 751, 500âĂŞ538, 2014.

[2] Murua J, et al. Applications of the Unsteady Vortex-Lattice Method in Aircraft Aeroelasticity and Flight Dynamics. *Progress in Aerospace Science*, DOI: 10.1016/j.paerosci.2012.06.001, 2012.

[3] Ramesh K, et al. Experimental And Numerical Investigations of Post-Flutter Limit Cycle Oscillations on a Cantilevered Flat Plate. *International Forum on Aeroelasticity and Structural Dynamics*, 2017.

[4] Hirato Y. Leading-Edge-Vortex Formation on Finite Wings in Unsteady Flow. North Carolina State University, 2016.

[5] Katz J. Discrete vortex method for the non-steady separated flow over an airfoil. *Journal of Fluid Mechanics*, 102(1), 315âĂŞ328, 1981.

[6] Katz P, Plotkin A. *Low-Speed Aerodynamics*. Cambridge University Press.

[7] Bisplinhoff R, et al. *Aeroelasticity*. Dover Publications INC.

6 Acknowledgements

This work was conducted during a scholarship supported by Brazilian Federal Agency for Support and Evaluation of Graduate Education (CAPES) within the Ministry of Education of Brazil at Instituto TecnolÃşgico de Aeronautica.

7 Author Contact Information

Tiago Priolli Monteiro
tiagopmonteiro@yahoo.com.br

Copyright Statement